I&EC research
Industrial & Engineering Chemistry Research

pubs.acs.org/IECR
Article

Iso-Potential Operando Microwave Cavity Perturbation–Spatial Conductivity Changes of a Cu/ZnO/Al_2O_3 Catalyst Inside a Fixed-Bed Reactor During Reverse Watergas Shift Reaction

Published as part of Industrial & Engineering Chemistry Research special issue "Smart Reactors—Towards Adaptive, Resilient, and Autonomous Process Systems".

Diego Espinoza, Neda Kazemi, Zoran Bondzio, Oliver Korup, Thomas Risse,* and Raimund Horn*

Cite This: https://doi.org/10.1021/acs.iecr.6c01137

ABSTRACT: This work explores the combination of Microwave Cavity Perturbation (MCP) with the concept of Iso-Potential Operando Spectroscopy (IPOS) to develop IPO-MCP for measuring conductivity changes in a catalyst within a catalytic fixed-bed reactor (FBR). As proof-of-concept, spatially resolved dielectric properties, species, and temperature profiles were recorded during the reverse water–gas shift (rWGS) reaction on a commercial copper–zinc-alumina (CZA) catalyst. These results reveal a linear electronic structure–activity relationship along the catalyst packing demonstrating that hydrogen significantly enhances the Q-value compared to carbon dioxide in line with previous investigations. This research motivates further application of IPO-MCP to other catalytic systems with distinct conductivity changes.

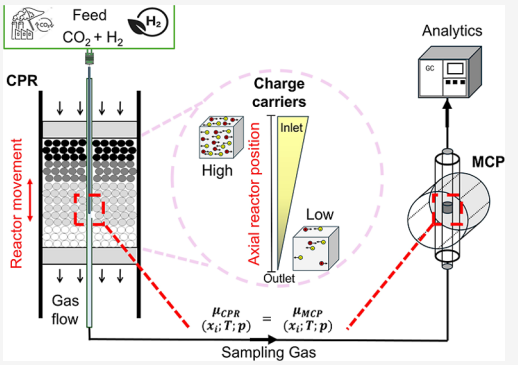

INTRODUCTION

As the global population continues to grow, the demand for chemicals that support modern living standards increases in parallel. This makes the development of sustainable production and usage strategies a priority for both science and industry.[1] Transitioning to renewable sources presents technological challenges, as raw materials and energy inputs fluctuate seasonally and geographically. In this context, heterogeneous catalysis plays a crucial role as it is estimated that 85–90% of all chemical products are manufactured using catalysts at some stage in their production.[2] Catalysis enables the conversion and storage of fluctuating renewable energy sources (e.g., solar and wind) into chemical energy carriers, such as green hydrogen produced by water electrolysis. Additionally, it allows for the use of atmospheric carbon dioxide as a renewable carbon feedstock, also known as Carbon Capture and Utilization (CCU).[3] A chemical reaction offering both benefits is the reverse water–gas shift reaction (rWGS). In this process, carbon dioxide (CO_2) reacts with hydrogen (H_2) to produce carbon monoxide (CO) and water (H_2O) (eq 1). Carbon monoxide serves as a building block that can be further transformed into high-value chemicals such as e-fuels and oxygenates. (e.g., via Fischer–Tropsch).[4]

$$CO_2 + H_2 \leftrightarrow CO + H_2O \quad \Delta H^0_{298K} = 41.3\text{kJ/mol} \qquad (1)$$

The rWGS reaction is endothermic; therefore, by Le Châtelier's principle, it becomes favorable at higher reaction temperatures (400–800 °C), making it an energy-intensive process.[4,5] Industrially, a 3:1 H_2:CO_2 feed is typically used to provide a 2:1 H_2/CO ratio for downstream processes such as methanol synthesis or Fischer–Tropsch. A detailed account on rWGS thermodynamics at low temperatures for this stoichiometry with and without CH_4 formation can be found in[6] and.[3] A plot of the thermodynamically achievable CO_2 conversion at low temperatures (190–240 °C), 100% CO selectivity and the 1:1 stoichiometry used in the present paper to demonstrate the IPO-MCP methodology is provided in the Supporting Information (Figure S3). In the low-temperature regime (200–250 °C), ternary Cu–ZnO–Al_2O_3 catalysts (CZA) have been demonstrated as a feasible solution. They are characterized by the low cost of copper (Cu), high activity to CO_2 activation, and high selectivity toward CO at atmospheric conditions; however, due to the thermodynamic challenges, CO_2 conversion remains a limiting factor.[5,7,8] Reaction

Received: March 12, 2026
Revised: May 29, 2026
Accepted: June 4, 2026

https://doi.org/10.1021/acs.iecr.6c01137
Ind. Eng. Chem. Res. XXXX, XXX, XXX–XXX

operation in the low-temperature regime can decrease operating costs and extend the lifespan of the CZA catalyst. Consequently, research aimed at improving CO_2 conversion at low temperatures would be valuable to support the global energy transition.[5,9]

ISO-POTENTIAL OPERANDO SPECTROSCOPY

The chemical industry must evolve fast to achieve sustainable industrial development that keeps pace with global population growth. Addressing this challenge requires rapid development of catalysts and catalytic reactors which can integrate fluctuating energy sources and variations in feedstock composition. Unlike process development during the last decades, which primarily relied on combinatorial trial-and-error methods, serendipity and incremental improvements,[10] a knowledge-based approach could accelerate this development by delivering solutions in a faster and more economical manner.[11−14]

The field of operando research has evolved to address the challenge of understanding catalytic processes by utilizing advanced experimental approaches and modeling. Understanding structure−activity relationships in heterogeneous catalysis requires a multimodal catalyst characterization using a variety of methods. Commonly probed aspects in operando catalysis research comprise the structural characterization of the catalyst bulk and surface, e.g. by X-ray Diffraction, Electron Microscopy and EXAFS, the detection of surface adsorbates, e.g. by Raman-Spectroscopy and DRIFTS, the electronic characterization of the catalyst bulk and surface e.g. by XANES, UV/vis, XPS and EPR, as well as the kinetic characterization, e.g. by SSITKA or TAP. No single method can provide the necessary information to develop a comprehensive mechanistic and kinetic understanding of the catalytic reaction. Each method provides only "puzzle pieces", which, when assembled, enable the derivation of structure−activity relations for a given catalytic system.

Operando spectroscopy enables researchers to capture a diverse range of information across various spatial and temporal scales by collecting data under relevant working conditions, rather than in simplified or ex-situ environments.[15,16]

The resulting high-quality data sets hold significant potential for validating and improving kinetic models and for facilitating systematic, knowledge-based optimization of catalyst materials. Additionally, incorporating the spatial dimension into operando research offers the advantage of providing localized information throughout the entire catalyst bed, thereby increasing data density, as each position corresponds to unique reaction conditions. Having more high-quality data can lead to shorter development times for processes and materials.[17,18] Despite significant advancements, conventional operando spectroscopy still faces fundamental challenges that limit its industrial application.[19] From the perspective of the authors, these limitations can be categorized into three main groups:[20]

1. Accessibility: Chemical reactors are nontransparent and opaque to electromagnetic radiation; they are made from stainless steel, with no optical access and operate under harsh reaction conditions (e.g., corrosive/explosive environment, high temperature and pressure).
2. Methodical: Classical operando spectroscopy cells are often kinetically ill-defined (dead volumes, bypass flows, undefined temperature measurements, blank activity, condensation of chemical components on unheated windows etc.).
3. Scientific: As temperature, pressure and chemical composition varies widely in catalytic reactors, it is unclear at which conditions an operando experiment should be conducted.

To tackle these challenges, a new approach for performing operando spectroscopy has recently been introduced, referred to as "Iso-Potential Operando Spectroscopy" or abbreviated "IPOS".

The technique developed by REACNOSTICS GmbH[21] enables operando spectroscopic measurements by combining spatially resolved concentration and temperature measurements in a profile reactor with operando spectroscopic measurements in a dedicated spectroscopic cell.

IPOS theoretically enables the study of solid catalysts in reactors of any size by any spectroscopic, microscopic, or imaging method that is compatible with the reaction conditions inside the reactor (e.g., DRIFTS, XRD, Raman, TEM). Measurement cells can be used which are optimized for the respective spectroscopic or microscopic method, without any design constraints resulting from the necessity to perform kinetic measurements in these cells. In a previous study, the IPOS approach was demonstrated for the first time by integrating it with DRIFTS to investigate surface adsorbates within a catalytic reactor during CO_2 methanation on a supported Ni/γ-Al_2O_3 catalyst.[20] The spatially resolved correlations between gas-phase chemistry and surface species suggested that methanation follows an associative mechanism under the conditions examined. Surface formate species, $*HCOO_{ads}$ were identified as a kinetically significant intermediate.

Charge carrier dynamics in the bulk of the catalyst and at the interfaces of the catalyst are an important yet less frequently studied aspect of many heterogeneous catalysts, especially those containing semiconducting materials. Microwave Cavity Perturbation (MCP) was developed to enable the noninvasive contactless determination of catalyst dielectric properties in a FBR.[22,23] The contactless design of the technique, via cavity resonator, solves the challenges of reproducible contact between electrode-catalyst (e.g., via sintering, water loss, and bed porosity), and the catalytic activity associated with conventional AC/DC metal electrodes.

This study evaluates the compatibility of the MCP technique with the IPOS methodology as a proof-of-concept. The method is named "Iso-Potential Operando MCP" and abbreviated as "IPO-MCP". The approach combines the noninvasive features of MCP with the versatility of the IPOS methodology, offering spatially resolved insights into the correlation of the catalysts dielectric properties with catalytic activity in a FBR.

As case study, an industrial CZA catalyst was investigated during the rWGS reaction. The chosen system offers two key advantages: First, CZA catalysts are essential for sustainable development because of their high efficiency, low cost, and widespread applications in environmentally significant processes aiming at CO_2 reduction, such as methanol synthesis and CO_2 hydrogenation. Second, this catalyst has been previously studied, providing supporting data to validate the proposed methodology.[7]

https://doi.org/10.1021/acs.iecr.6c01137
Ind. Eng. Chem. Res. XXXX, XXX, XXX−XXX

MICROWAVE CAVITY PERTURBATION (MCP)

The MCP method was developed for the contactless measurement of electrical conductivity and complex permittivity, which allows exploring electronic structure−function relationships in materials science and heterogeneous catalysis. In catalysis research it is used as an in situ or operando tool which relies on the perturbation of a resonance mode within a microwave cavity when the complex permittivity of a catalyst is altered.[7,24,25] To this end, a sample is placed in the microwave cavity such that it interacts with the electric field component of the standing wave pattern. A Vector Network Analyzer (VNA) is used to excite the resonance mode and record the complex valued reflection coefficient, as defined in eq 2. In case the incident microwave matches the resonance frequency of the cavity, the energy from the incident wave (V_+) is stored in the cavity leading to drop of the reflected wave (V_-). The properties of the cavity can be characterized by the so-called reflection coefficient

$$|\Gamma(\omega)| = \frac{V_-}{V_+} \tag{2}$$

Its frequency dependence, known as the reflection curve, allows for the quantification of the properties of a cavity. A commonly used parameter is the quality factor (Q-factor), a dimensionless parameter quantifying the ability of the cavity to store energy. It is defined by the ratio between the resonance frequency and the spectral width of the mode at half height according to eq 3 (s. also Figure 1).

$$Q = \frac{\omega_{\text{res}}}{\Delta\omega_{1/2}} \tag{3}$$

Since the ability of a cavity to store energy, as characterized by its Q-value, is directly linked to its dielectric losses, introducing an absorbing material or changing its dielectric properties will alter the Q-value. Figure 1 schematically illustrates the changes of the resonance mode when loading an absorbing material into a microwave cavity. The Q-value is extracted from the reflection curves by fitting the complex reflection coefficient. More details can be found in the literature.[24]

ISO-POTENTIAL OPERANDO MICROWAVE CAVITY PERTURBATION (IPO-MCP)

Figure 2 illustrates the IPO-MCP working principle employed in this study for the non-invasive measurements of catalysts dielectric properties in a FBR. In general, IPOS aims to approximate the local chemical potential in the catalytic reactor ($\mu_{\text{CPR}} = f(T,p,x)$) to match that in the spectroscopic device; in this case, the MCP cavity ($\mu_{\text{MCP}} = f(T,p,x)$). The process is experimentally conducted using a Compact Profile Reactor (CPR) for spatially resolved concentrations and temperature measurements.

In the CPR, a stainless steel or fused silica capillary with up to four side sampling orifices, laser-drilled at a certain axial position in the capillary wall, is fixed in space and runs through the center of the reactor tube holding the catalyst bed. A thermocouple located inside the sampling capillary and tip-aligned with the sampling orifices enables direct temperature measurement at the sampling position. By shifting the catalyst bed laterally along the sampling orifice, composition and temperature profiles can be recorded. The locally sampled reaction mixture is then transferred from the reactor to the

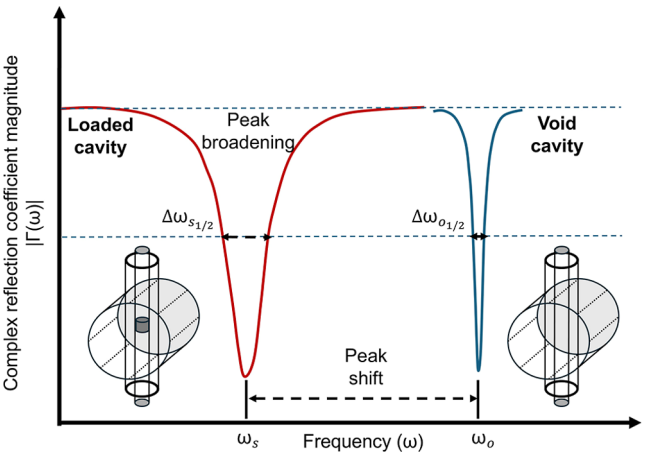

Figure 1. Working principle of Microwave Cavity Perturbation (MCP). The reflection loss plot illustrates the shift in resonance frequency (ω_s−ω_o) and peak broadening ($\Delta\omega_{s1/2}$−$\Delta\omega_{o1/2}$) by introducing a powder catalyst sample in the cavity resonator. Adapted with permission from.[24] Copyright 2012 Wiley-VCH Verlag GmbH & Co. KGaA, Weinheim.

microwave cavity, where a small amount of the same catalyst as in the reactor is placed. The Gas Hourly Space Velocity (GHSV) in the MCP cavity is kept as high as possible, at least ten times the value at the exit of the catalyst bed in the CPR, such that catalytic conversion in the MCP cavity is as small as possible exposing the catalyst in the MCP cavity to approximately the same chemical composition (x) as the catalyst at the place of sampling in the CPR. By further keeping the pressure drop in the transfer line negligible and by adjusting the temperature of the catalyst in the MCP cavity to the same value as measured locally at the sampling position, the catalyst in the MCP cavity is in good approximation exposed to the same temperature (T), pressure (p), and composition (x) as the catalyst at the chosen position of the orifice inside the catalyst bed. By matching the chemical potential, the catalyst characterized spectroscopically should exhibit the same reactivity and electronic structure as the catalyst in the reactor bed at the position of interest, allowing for a spatially resolved measurement of the property of interest, in this case, the dielectric loss function of the catalyst. More details on IPOS can be found in the experimental section and previous publications by the authors.[20,21]

EXPERIMENTAL SECTION

The IPO-MCP methodology is based on the principles of matching temperature (T), pressure (p), and chemical composition (x) between the reactor and the spectroscopic device. To achieve this, the workflow of this study was organized into two main stages.

In the first stage, the dependence of the cavity Q-factor on contact time in an end-of-pipe operando MCP experiment during rWGS reaction was explored to (i) minimize conversion in the spectroscopic cell, hence approaching iso-potential conditions, and (ii) ensure a sufficient signal-to-noise ratio in the microwave cavity Q-factor. Initial screening of temperature and flow conditions was performed to establish a composition gradient across the entire CPR bed. Spatially resolved temperature profiles indicated isothermal behavior (T). Additionally, extended on-stream experiments confirmed the stability of the catalyst.

In the second stage, the integration of the CPR and MCP device was performed. Pressure gradients between devices were minimized (p). Finally, spatially resolved conductivity measurements (IPO-MCP) were conducted following the previously established

https://doi.org/10.1021/acs.iecr.6c01137
Ind. Eng. Chem. Res. XXXX, XXX, XXX−XXX

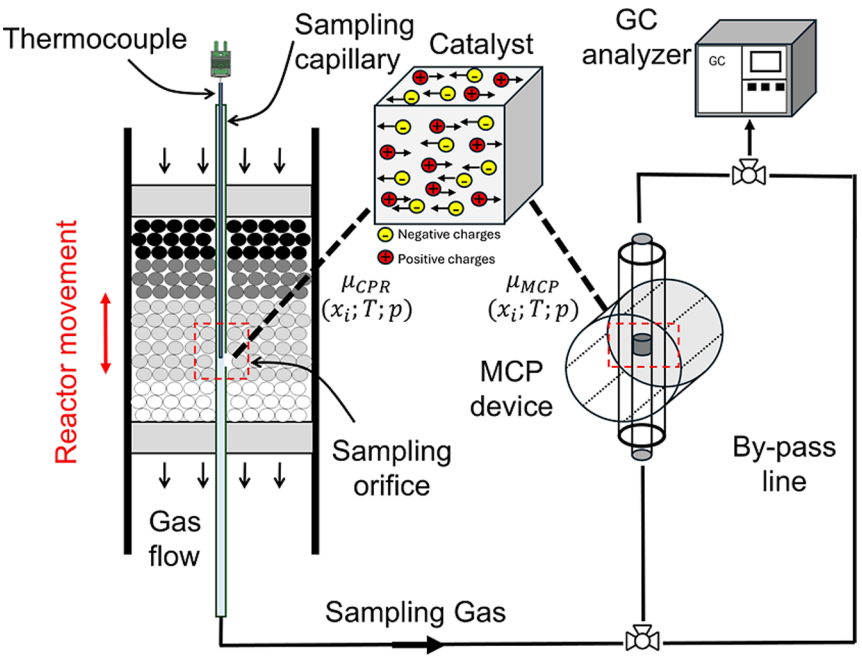

Figure 2. Schematic of the IPO-MCP experiment for spatially resolved operando conductivity measurements in a FBR.

experimental conditions. Further details are provided in the experimental section.

Catalyst Characterization

A commercial $Cu/ZnO/Al_2O_3$ (CZA) catalyst (CM4009, Stanford Advanced Materials) was utilized to conduct the rWGS experiments. Before IPO-MCP measurements, the catalyst was characterized by powder XRD, elemental analysis (ICP), and surface area evaluation (BET).

High-energy X-ray total scattering experiments were performed in the experimental hutch of the Beamline P21.1 at PETRA III (DESY, Hamburg). The samples were mounted in a 0.5 mm inner diameter glass capillary. A 1 × 1 mm^2 beam was used at 101.5 keV. Scattering data were collected on a Pilatus3 CdTe detector positioned at a sample-to-detector distance (SDD) of 1100 mm.

To calibrate the SDD and remaining detector geometry parameters, a capillary containing LaB_6 powder was used as standard. Azimuthal integration of the 2D diffraction patterns and calibration were carried out using the pyFAI package. Elemental analysis of the catalyst was carried out using inductively coupled plasma-optical emission spectroscopy (ICP-OES) on an Optima 8300 DV (PerkinElmer). The specific surface area of the catalyst was measured by N_2 physisorption using standard BET analysis with an Autosorb iQ device (Quantachrome). Results were compared with values provided by the manufacturer.

Stability and Reproducibility Tests

In the first experimental step, the catalytic performance and stability of the rWGS reaction over a $Cu/ZnO/Al_2O_3$ (CZA) catalyst were evaluated using a Compact Profile Reactor (CPR 5.0, REACNOSTICS GmbH). The CPR allows for the determination of concentration and temperature gradients within the catalytic fixed bed using the capillary sampling. A stainless steel or quartz capillary (OD 700 μm, ID 520 μm) is located in the center of the catalyst bed, featuring side sampling orifices at a certain axial position of the capillary, through which gas samples are continuously extracted and analyzed. In the present work, a stainless-steel capillary with four side sampling orifices of 50 μm diameter was used. A type-K thermocouple (OD 250 μm) (TMH GmbH) is located inside the capillary, tip-aligned at the position of the orifices, for local temperature measurements.[17] Gas dosing was performed by a set of mass flow controllers (EL-FLOW Select, Bronkhorst GmbH). Reaction mixture quantification was achieved by a mass spectrometer (HPR 20, Hiden), equipped with a Faraday cup detector and a heated capillary inlet. Multiple Ion Detection (MID) was employed to evaluate the mass-to-charge ratios (m/z) of H_2 (2), Ar (40), and CO_2 (44). Selectivity to CO on this CZA catalyst in this study was close to 100%, such that the system could be represented by a single stoichiometric equation (eq 1). The reaction products, CO and H_2O, were calculated based on the stoichiometry of the rWGS reaction.

Catalytic stability tests were conducted by packing the CZA catalyst into the CPR reactor tube (OD 6 mm, ID 4 mm) using a sieve fraction of 300−400 μm, resulting in a bed length of 50 mm. The catalyst was activated by flowing a reducing gas mixture of H_2 and Ar with a volumetric ratio of 5:95 through the catalyst bed. The temperature gradually increased from room temperature to 250 °C at 1.2 °C min^{-1}, followed by a 90 min hold at 250 °C. Once activation was complete, the temperature of the catalyst was adjusted to 225 °C, and the feed was changed to the reaction gas mixture of H_2, CO_2, and Ar in a volumetric ratio of 10:10:80. Both catalyst activation and reaction were conducted with a total flow rate of 100 mL min^{-1} (adjusted at 25 °C, 1 atm). Prior to profile measurements, the system was running for 1 h at these conditions to reach steady state. After this, concentration profiles of the species were measured at 10 positions along the catalytic bed, spaced 6 mm apart. Three profile replicates were measured in total.

Operando MCP stability measurements were carried out using an Agilent PNA-LN5230C vector network analyzer (VNA) connected to a cylindrical silver and gold-plated resonator (34 mm in radius; 20 mm in height, TM_{020} mode, 7.1−7.37 GHz) with a MW power attenuation of 5 dBm. MCP stability measurements were conducted by packing the CZA catalyst (sieve fraction 100−200 μm) into the cavity reactor tube (ID 3 mm), resulting in a bed length of 5 mm. An initial operando MCP experiment using the 300−400 μm sieve fraction failed due to instability of the catalyst bed. Since the catalyst serves as a sensing element for the local chemical potential in any IPOS application, the fixed bed was packed with a 100−200 μm sieve fraction of the catalyst, as this had previously been found to result in stable measurement conditions.

In the MCP cavity reactor, catalyst activation was conducted by flowing a reducing gas mixture of H_2 and Ar (5:95) through the cavity reactor tube. This process was performed by heating the reactor to 250 °C at 1.2 °C min^{-1}, then holding at 250 °C for 90 min. Following activation, reflection curves were measured during the rWGS reaction as a function of contact time.

https://doi.org/10.1021/acs.iecr.6c01137
Ind. Eng. Chem. Res. XXXX, XXX, XXX−XXX

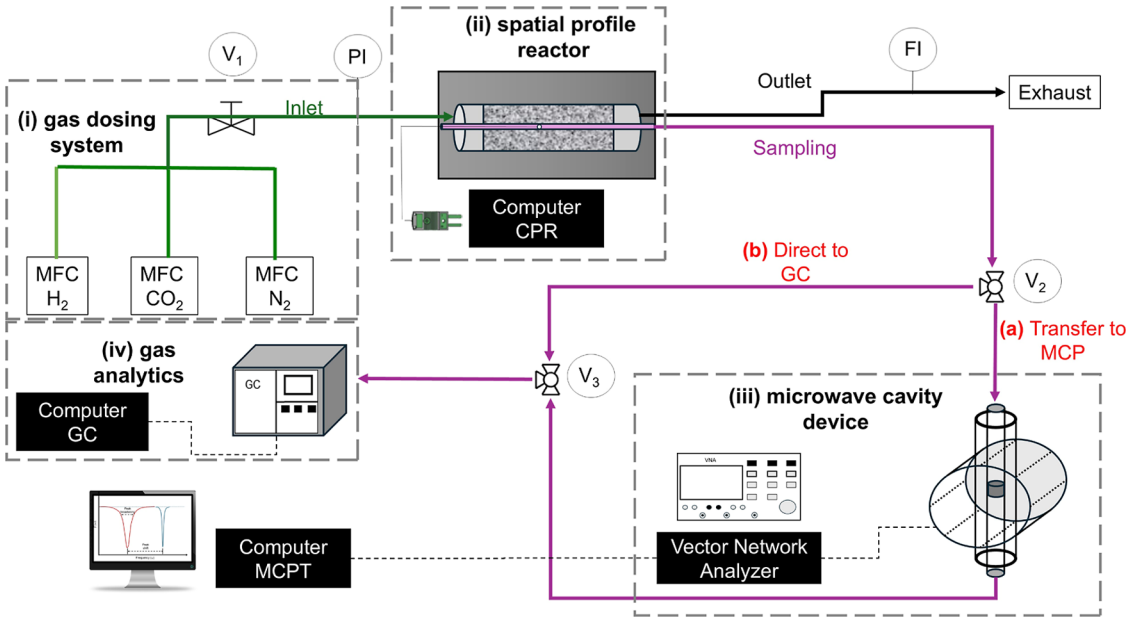

Figure 3. Diagram of the main components for the IPO-MCP experimental setup. (i) MFCs, (ii) Compact Profile Reactor (CPR), (iii) MCP and VNA device, (iv) Gas analytics system (GC). The proposed valve configuration allows an in-series connection of the CPR sampling line with the MCP (route-a) or bypassing of the cavity (route-b).

To establish the correlation between reactivity and Q-values, measurements were conducted at different GHSVs ranging from 11571 mL g_{cat}^{-1} h^{-1} to 88714 mL g_{cat}^{-1} h^{-1}. Reflection curves were continuously recorded and averaged resulting in a temporal resolution of 1 min.

ISO-POTENTIAL Operando MCP Profiling

In the second step, IPO-MCP measurements were performed by coupling the CPR and the MCP functionalities as described above. The methodology allows simultaneous investigation of the local electronic structure of the CZA catalyst and its reactivity during the rWGS reaction in a FBR. The entire experimental setup is schematically illustrated in Figure 3. The setup consists of four main components: (i) a gas dosing system, (ii) a spatial profile reactor, (iii) a microwave cavity device (MCP), and (iv) gas analytics.

The profile reactor and gas dosing system used in step two were the same as in step one, with the only difference that in step two, gas analysis was conducted using a gas chromatograph (GC) (Agilent 7890A) equipped with a catalytic microreactor (polyarc) to convert carbon containing gases into methane, detected by a subsequent flame ionization detector (FID). CPR and MCP were connected using a heated transfer line (Hillesheim GmbH), the length of which was kept to a minimum to reduce pressure drop between the reactor and the cavity. Sampling valves and transfer lines were heated for the measurement of condensable species.

To approach iso-potential conditions, the GHSV ratio between the cavity and the CPR-reactor was maximized to minimize CO_2 conversion in the MCP cell and get as close as possible to the chemical potential locally in the CPR. There is no general rule in IPOS for how much sampling volume must be extracted from the CPR and how much catalyst must be put in the spectroscopic cell. The GHSV value that can be realized in the spectroscopic cell depends on the rate of the catalytic reaction, the total flow rate in the reactor, and the sensitivity of the measurement method. As a rule of thumb, the GHSV in the spectroscopic cell should be at least 1 order of magnitude higher than at the outlet of the catalyst bed. Under these conditions, the conversion in the spectroscopic cell remains below one-tenth for zeroth-order kinetics (and even lower for higher reaction orders). In addition, the flow rate withdrawn from the CPR through the sampling capillary should not exceed 20% of the total reactor flow to minimize disturbances of the flow conditions in the catalyst bed downstream of the sampling orifices. In the IPO-MCP experiments in the present work, the sampling flow rate through the transfer line was initially set to 20% of the total flow through the CPR using a micrometer needle valve (Vici Valco GmbH) equipped with a heating jacket (Horst GmbH). Next, the catalyst mass in the microwave cavity was selected to balance the MCP signal-to-noise ratio with the catalytic conversion in the MCP reactor. Finally, a selection valve system was used to direct the sampled gas either directly to the GC or to the MCP device to evaluate the additional conversion caused by the MCP cavity and the catalyst therein. Since factors such as total mass, bed packing, and relative position in the cavity field influence the Q-value, the CZA catalyst was not replaced in between measurements, allowing the neglect of these effects. The Q-value from the activation stage (H_2/N_2/5:95 at 250 °C) was used as a reference point for further comparisons, and the term ΔQ is defined as the difference between the Q-value under reaction conditions (Q_{rxn}) and reference state (Q_{act}) according to eq 4 (Table 1).

$$\Delta Q = Q_{rxn} - Q_{act} \tag{4}$$

Table 1 summarizes the relevant experimental parameters used to implement the IPO-MCP methodology. Prior to profile measurements, both the reactor and the cavity were heated simultaneously to 225 °C at a rate of 2.4 °C min^{-1} under reducing conditions (5 vol % H_2 in N_2). Once the target temperature was reached in both devices,

Table 1. Experimental Operational Parameters Employed During IPO-MCP Measurements

Experimental parameter	Units	CPR	MCP
Temperature $_{set}$	°C	225	-
Temperature $_{capillary}$	max	213.5	-
	min	212.1	-
	average	213	213
Pressure	bar	1.6	1.4
Mass of catalyst	g	0.662	0.014
Particle size	μm	300−400	100−200
Bed length	mm	50	5
Flow (25 °C, 1 atm)	mL min^{-1}	100	20
GHSV	mL $gcat^{-1}$ h^{-1}	9058	85714

https://doi.org/10.1021/acs.iecr.6c01137
Ind. Eng. Chem. Res. XXXX, XXX, XXX−XXX

the gas feed was switched to the reaction feed, and the system was allowed to stabilize for 1 h. Spatially resolved measurements were performed at 10 positions along the reactor. In the inlet/outlet region of the quartz wool, a step size of 2.5 mm was employed; inside the catalytic bed, a step size of 10 mm.

The catalytic stability and reversibility of the system were assessed by changing the sampling direction. In IPOS, the chemical history of the catalyst in the spectroscopic cell should reflect the chemical history in the reactor as closely as possible. While it is unavoidable that the time, during which the catalyst in the reactor and in the spectroscopic cell are exposed to a certain chemical environment differ, scanning from reactor inlet to outlet ensures that the catalyst in the spectroscopic cell proceeds through the same sequence of chemical potentials as the catalyst in the reactor from the beginning of the catalyst bed to the end. To account for the different time-stamps, sufficient time must be given to the catalyst in the spectroscopic cell to complete all changes, be they reversible or irreversible. If all catalyst changes are reversible, measuring from outlet-to-inlet will give the same reactor and spectroscopic profiles as from inlet-to-outlet. If some catalyst changes were irreversible (e.g., sintering, poisoning, fouling), reactor and spectroscopic profiles measured from outlet-to-inlet would differ from those measured from inlet-to-outlet, and only the latter should be considered. The degree of reversibility can also be probed by repeated scans from inlet-to-outlet, but as it takes time to scan the reactor, it is always recommended to record the data "on the way back". In the present work, both reactor profiles and ΔQ profiles were independent of the scan direction, indicating a high degree of reversibility of this particular catalytic system under the explored reaction conditions. In total, four profiles were measured while maintaining the same reaction conditions. Two profiles, one with and one without the MCP cavity, were measured by sampling from reactor inlet-to-outlet (forward sampling scheme) and two profiles were measured from reactor outlet-to-inlet (backward sampling scheme), again with and without the MCP cavity.

RESULTS AND DISCUSSION

Catalyst Characterization

The metal loading of the precatalyst determined by ICP-OES was 50.4/9.2/3.2 wt % for Cu/Zn/Al, respectively. Ex-situ XRD measurement (Figure S1) of the powder CZA catalyst sample before activation exhibited diffraction patterns in the range of 1 to 6° (2θ) using high-energy X-rays (λ: 0.12215 Å). The highest intensities correspond to ZnO and CuO phases. The peaks at 2.75° are indexed to the (002) and (101) planes of hexagonal wurtzite ZnO, respectively. Additionally, peaks at 3° (2θ), correspond to the (111) planes of monoclinic CuO (tenorite). Although most components showed characteristic reflections of CuO and ZnO, the zincian malachite phase also contributed to the diffraction pattern, with peaks observed between 1.4 and 2.3° (2θ). These phases can be decomposed into the active catalyst species through thermal treatment or reduction processes. BET measurements yielded a surface area of 89 $m^2\ g^{-1}$ and a pore volume of 0.25 mL g^{-1}, in fair agreement with the manufacturer's values of 70 $m^2\ g^{-1}$ and 0.17 mL g^{-1}.

Stability and Reproducibility Tests

Figure 4 illustrates the spatially resolved concentration and temperature profiles within the catalytic FBR during the rWGS reaction over a CZA catalyst. The reaction mixture consists of CO_2 and H_2 as reactants, with CO and H_2O as the main products. Quartz wool plugs were used to secure the catalyst bed at both the inlet and outlet zones, creating an entrance region from −10 mm to 0 mm where no catalytic activity is observed. The catalyst bed begins at position 0 mm, which is the point where CO_2 starts to react with H_2. As the gas mixture

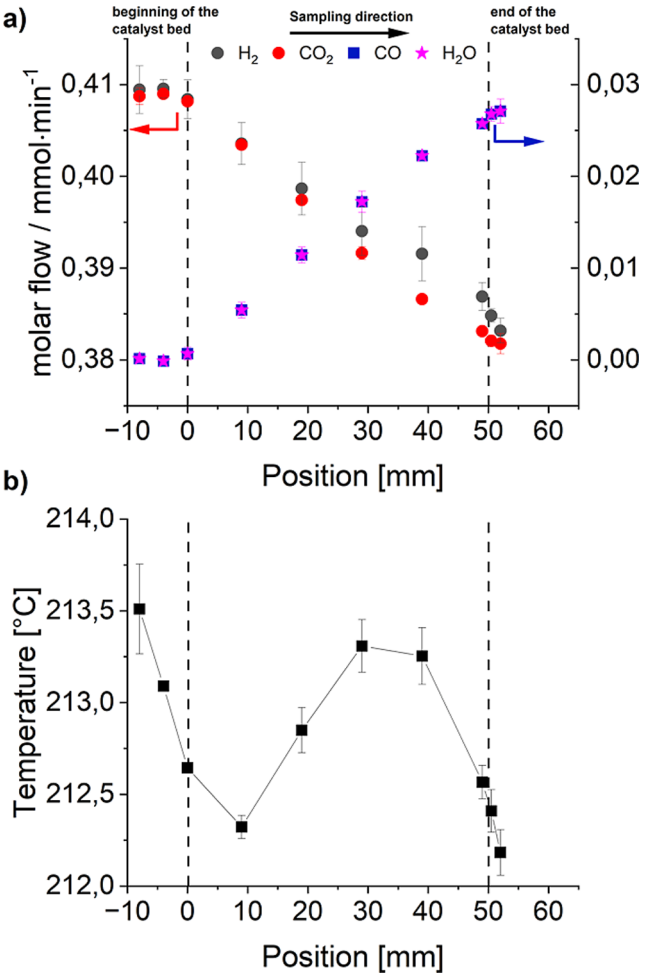

Figure 4. (a) Spatially resolved species concentration profiles of reactants (CO_2 and H_2) (Left Axis) and products (CO and H_2O) (Right axis). (b) Temperature profiles with standard deviation obtained during rWGS reaction over an industrial CZA catalyst. Reaction conditions: Feed composition $CO_2/H_2/Ar$ = 10/10/80, T_{set} = 225 °C, 100 mL min^{-1} (25 °C, 1 atm), 3 replicates, and 50 mm catalyst bed.

flows through the bed, CO_2 and H_2 concentrations decrease while CO and H_2O increase. Even though the reactor is placed inside a temperature-controlled heating block, the endothermic nature of the reaction is partially evident in the temperature profile (Figure 4b), as the gas temperature initially declines slightly along the catalyst bed, reaching a minimum at 10 mm, being about 1 °C lower than the temperature at the entrance. While the temperature rises for the next 20 mm and drops at the end of the reactor, the temperature variations within the reactor stay below 1 °C, indicating an acceptable isothermal behavior throughout the catalyst bed. The reaction products CO and H_2O increase linearly along the bed for about 30 mm to 40 mm, showing a slightly reduced slope near the exit region (50 mm to 60 mm), most likely due to the reaction approaching thermodynamic equilibrium. Overall, there is good agreement across replicates, providing reliable proof of stable catalytic performance under the conditions of this study.

Figure 5 shows a stand-alone operando MCP measurement of the CZA catalyst as a function of contact time without coupling the MCP cell to the profile reactor. The catalyst was activated according to the protocol described above. Reducing the contact time leads to a reduction of the CO yield as well as

https://doi.org/10.1021/acs.iecr.6c01137
Ind. Eng. Chem. Res. XXXX, XXX, XXX−XXX

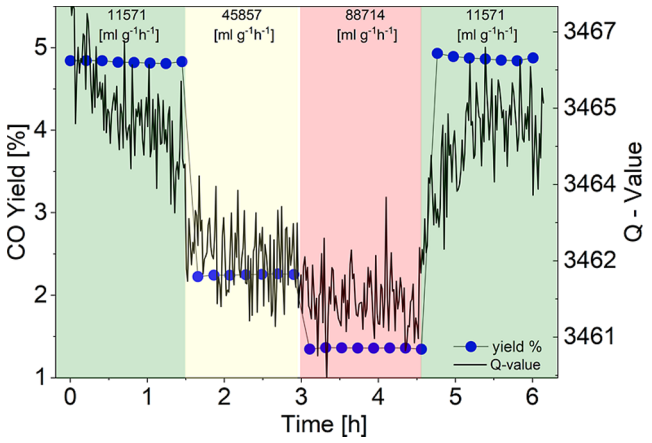

Figure 5. Contact time dependent operando MCP measurement during rWGS experiments. Reaction conditions: $CO_2/H_2/N_2$ = 10/10/80, T_{set} = 218 °C. Screening GHSV range: 11570 to 88714 mL g_{cat}^{-1} h^{-1}.

the Q-value. Importantly, both catalytic activity and Q-value are perfectly reversible if going back to the initial contact time at the end of the experiment. This observed reversibility is in agreement with previous investigations.[7] In this study, the addition of H_2 and CO_2 was shown to decrease and increase the Q-value, respectively, which is associated with the ability of the two reactants to donate (H_2) or abstract (CO_2) electrons into or from the system. In case of H_2, the change in Q-value is reversible even in the absence of CO_2, which shows that it is due to a physical dissolution of hydrogen in the system and not a chemical reduction associated with a loss of oxygen in the system. In contrast to that, an activated catalyst reduces CO_2 to CO, and the associated increase of the Q-value is completely irreversible in the absence of hydrogen and is due to an oxidation of the activated catalyst. During the catalytic rWGS reaction, Asadi et al., 2025 demonstrated that the system could transiently store oxygen, the quantity of which depended on the CO_2 chemical potential in the gas phase. For the CO_2 pressure used here, the transient amount of oxygen is less than 1 mol % of the total oxygen content. Importantly, the amount of dissolved H_2 is also determined by the chemical potential of H_2 in the gas phase. While the change of Q-value scales linearly with CO yield for both reactants (H_2 and CO_2), for a given CO yield, the change is larger for the H_2 dependence, which explains the reduced Q-value shown in Figure 5 for reduced CO_2 conversion, hence, higher partial pressure of H_2 and CO_2 in the gas mixture.

ISO-POTENTIAL Operando MCP Profiling

Figure 6 illustrates the spatially resolved rWGS electronic structure−activity data within a catalytic FBR obtained by the IPO-MCP methodology. The methodology provides three key pieces of information: (i) the spatially resolved carbon monoxide (CO) yield, which reflects the catalytic activity of the CZA catalyst (Figure 6, right axis), (ii) the reactor temperature profile (Figure S2), and (iii) the spatially resolved dielectric changes of the CZA catalyst, indicated by variations in the cavity quality factor (ΔQ) (Figure 6, left axis). In contrast to the previous MCP pretests, temporal variations (e.g., residence time) are now translated into spatial variations, or an equivalent reactor coordinate. Spatially resolved scanning allows for obtaining structure−activity information across a

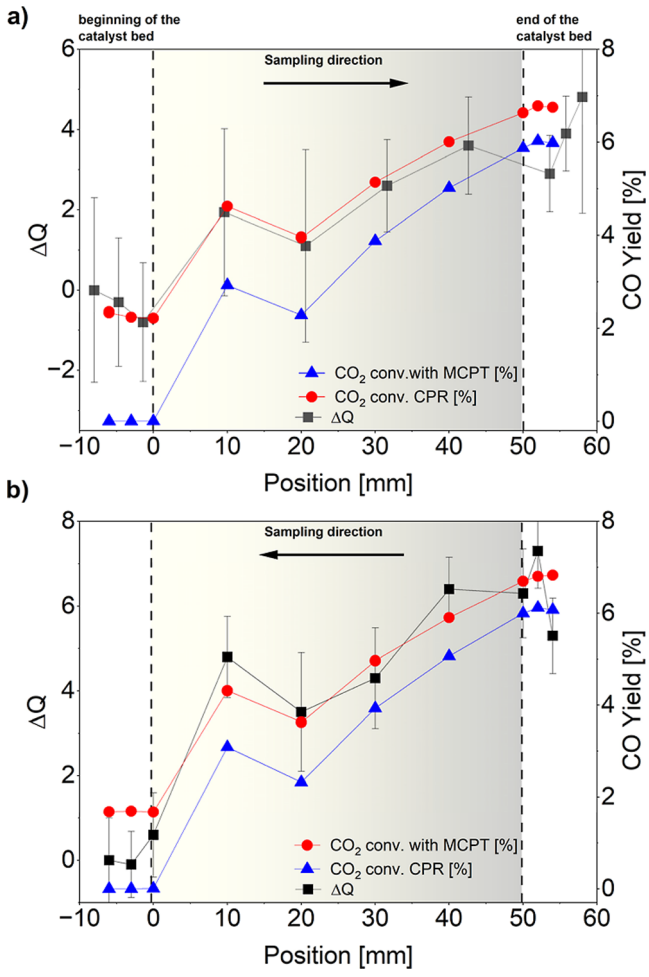

Figure 6. IPO-MCP profiles show the spatial correlation between dielectric properties and catalytic activity of a CZA catalyst during rWGS reaction. Replicates were included to evaluate the "in-sequence activity" under both scenarios: with (red curve) and without (blue curve) MCP integration. Left axis: Spatially resolved gradients in cavity factor ΔQ. Right axis: Spatially resolved CO yield profile. (a) Profiles measured using an "in-to-out" sampling scheme, and (b) Profiles measured using an "out-to-in" sampling scheme. Reaction conditions: Feed composition $CO_2/H_2/N_2$ = 10/10/80, T_{set} = 225 °C, 100 mL min^{-1} (25 °C, 1 atm), and 50 mm catalyst bed.

wider range of contact times within the same experiment by simply translating the sampling orifice position.

The successful application of the IPOS methodology relies on two main considerations covering the spatial and temporal domains. The first aspect consists of establishing locally quasi-iso-potential conditions between the profile reactor and the spectroscopy device. In an ideal case, in-series integration of the MCP with the CPR should not introduce any additional catalytic activity. However, this represents a theoretical limit that can never be reached, but research has shown that it can be closely approached in practical scenarios.[20] The second aspect requires evaluating the "memory effect" of the catalyst, which refers to its chemical history. In an ideal scenario, the catalyst's dielectric properties change reversibly in response to changes in the reaction feed. In a "forward" sampling scheme, also known as "in-to-out," the catalyst in the spectroscopic cell is exposed to the same sequence of chemical potentials over time as the catalyst in the reactor. Conversely, in a "backward" sampling scheme, or "out-to-in," the catalyst in the

https://doi.org/10.1021/acs.iecr.6c01137
Ind. Eng. Chem. Res. XXXX, XXX, XXX−XXX

spectroscopic device observes the conditions starting at the outlet of the reactor. Depending on conversion, these conditions may differ significantly from the feed conditions, leading in some cases to irreversible changes in the catalyst. To assess whether both conditions are fulfilled, we measured the "in-sequence activity" of the system by evaluating the CO yield both with and without the MCP cavity. Additionally, the reversibility of changes in dielectric properties and reactivity was examined through forward and backward profile measurements.

In line with previous stability experiments, the concentration and temperature profiles of the rWGS process follow the same chemistry previously discussed. Quartz wool plugs mark the entrance and exit zones of the catalyst bed, where no catalytic activity takes place. As the reaction mixture enters the catalyst bed at 0 mm, CO_2 is reduced by H_2, leading to a nonmonotonic increase in CO along the reactor axial length until 50 mm. Beyond this point, the outlet zone begins, leading to a plateau in catalytic activity. Throughout the reactor, axial temperature variations remained below 1 °C, validating the isothermal conditions assumed for operation of the MCP cavity resonator. However, isothermicity is no requirement for IPOS in general or for IPO-MCP in particular; it would work just as well if there were a pronounced axial temperature in the profile. The only additional requirement in this case would be to trace the local temperature in the spectroscopic cell as measured in the profile reactor, either by adjusting it manually or better in an automated way. An example of nonisothermal IPO−DRIFTS is presented in Sichert et al., 2024.

Additionally, Figure 6 (a) shows the difference in CO_2 conversion achieved by connecting the CPR in series with the MCP (represented by the red curve) compared to using only the CPR (shown by the blue curve). At the entrance of the catalyst bed at $z = 0$, a CO_2 conversion of 2% was measured "in-sequence", viz. with CPR and MCP cell connected in series. Considering that the overall conversion at the end of the bed is only 6%, this seems, at first glance, to be a fairly high deviation. However, if the chemical potential of the gas mixture is calculated at the entrance of the CPR ($Ar/CO_2/H_2/CO/H_2O$ = 0.8/0.1/0.1/0/0) and compared to the chemical potential in the MCP cell at 2% conversion ($Ar/CO_2/H_2/CO/H_2O$ = 0.8/0.098/0.098/0.002/0.002), the deviation in chemical potential is only about 1.5% (μ_{mix}^{CPR} = -40248 J mol^{-1} vs $\mu_{mix}^{CPR-MCP}$ = −40843 J mol^{-1}). At the exit of the catalyst bed, the deviation is even lower, as the additional small conversion in the MCP cell becomes less and less important.

MCP measurements complement the conversion profiles in Figure 6 by providing insight into the electronic structure of the CZA catalyst along the reactor. As shown in Figure 6 (black squares), the Q-value increases when moving toward the end of the catalyst bed in the CPR. This increase is directly correlated with the increase in CO yield. This result is in line with expectations based on previous observations. As shown above, larger contact times (low GHSV) associated with higher CO yield results in a higher Q-value, while short contact times leading to low CO yield and, in turn, higher partial pressures of H_2 and CO_2 result in lower Q-values. A closer examination of the position at 20 mm reveals a correlated decrease in Q-value and CO yield in both profiles. This decrease is not an artifact, but a real observation. Local variations in particle compaction may have resulted in differing porosities, leading to mixing in from gas from the slip flow region of the packing, as already observed in previous work e.g.,[26] and possibly a lower sampling volume in the CPR-MCP transfer system. As a result, the absolute FID detector response is slightly reduced at this position. From an electronic structure perspective, an increase in Q-factor along the catalyst bed implies a decrease in excitable charge carriers in the CZA catalyst. As discussed in the previous section, the amount of excitable charge carriers introduced into the system by H_2 is determined by the chemical potential in the gas phase. The chemical potential also determines the number of transiently stored oxygen atoms acting as sinks for excitable charge carriers. While both effects are present simultaneously during the rWGS reaction, the net effect for an equimolar ratio of the two gases is a decrease in the Q-value because of the leading effect of H_2 for these conditions.

The measured profiles indicate that variations in dielectric properties, specifically the Q-value, are reversible and independent of the sampling direction. Interestingly, even small variations in the local composition correspond to Q-value changes (dip at position 20 mm), highlighting the sensitivity of the MCP method. The results suggest that even when the CZA catalyst is subjected to different sequences of conditions, whether forward or backward sampling, its response remains consistent and is solely influenced by the current local composition. In other words, the CZA catalyst exhibits no "memory effect" under the conditions of this experiment. During iso-potential sampling, the time the catalyst in the spectroscopy cell is exposed to a particular chemical potential is generally shorter than the time it experiences in the reactor. In this experiment, a 15−20 min time interval between measurements was allowed to let the system stabilize. Previous studies have shown that the CZA catalyst reaches a new steady state within 10 min, which is consistent with the stable operation we observed.[7]

CONCLUSIONS

This work presents a proof-of-concept demonstrating the compatibility of MCP with the IPOS approach. The application range of operando MCP was expanded by providing, for the first time, spatially resolved information on dielectric properties in a fixed-bed reactor. The versatility and validity of the "iso-potential concept" were also demonstrated. Overall, the IPO-MCP methodology reveals both gas-phase activity and the local electronic structure of an industrial CZA catalyst during rWGS reaction. A linear correlation between dielectric properties and CO yield was observed as a function of reactor position, highlighting the connection between dielectric properties and catalytic performance. Previous studies support these findings and offer a theoretical framework for interpreting the observed spatial gradients in Q-values. Changes in the dielectric properties are mainly affected by the partial pressures of the reactants (H_2 and CO_2) along the reactor bed. H_2 is characterized by its ability to donate electrons, leading to a lower. Q-value, whereas CO_2 acts as a charge sink, increasing Q-value. During rWGS, H_2 has a more significant effect on the Q-value than CO_2, resulting in an overall increase in Q-value as both H_2 and CO_2 are consumed along the catalytic bed.

The proposed methodology serves as a basis for future research, covering the extension of the setup to new catalytic applications. While the current IPO-MCP setup operates near atmospheric pressure, the methodology could be extended to higher pressures; recent literature demonstrates that, with appropriate setup modifications, resonant cavity measurements

https://doi.org/10.1021/acs.iecr.6c01137
Ind. Eng. Chem. Res. XXXX, XXX, XXX−XXX

can be performed at industrially relevant pressures.[27] From a case-study perspective, periodic feed reactor operation could be employed as a strategy to address thermodynamic limitations by optimizing the uptake times of hydrogen (H) and oxygen (O) within the CZA structure. Additionally, other reaction systems, such as the selective oxidation of alkanes, where dielectric properties are known to influence alkene selectivity, could be studied in a spatially resolved manner.

■ ASSOCIATED CONTENT

Supporting Information

The Supporting Information is available free of charge at https://pubs.acs.org/doi/10.1021/acs.iecr.6c01137.

Supporting Information Structural (XRD) and elemental (ICP) catalyst characterization information. Temperature profiles obtained during IPO-MCP measurements (PDF)

■ AUTHOR INFORMATION

Corresponding Authors

Thomas Risse − *Institute of Chemistry and Biochemistry, Freie Universität Berlin, Berlin 14195, Germany*; Phone: +49 (0) 30 838 55313; Email: risse@chemie.fu-berlin.de

Raimund Horn − *Department of Chemical Reaction Engineering, Hamburg University of Technology, Hamburg 21073, Germany; Reacnostics GmbH, Hamburg 20457, Germany*; orcid.org/0000-0001-8457-3161; Phone: +49 (0) 40 42878 3042; Email: horn@tuhh.de

Authors

Diego Espinoza − *Department of Chemical Reaction Engineering, Hamburg University of Technology, Hamburg 21073, Germany*; orcid.org/0000-0002-0475-8121

Neda Kazemi − *Department of Chemical Reaction Engineering, Hamburg University of Technology, Hamburg 21073, Germany*

Zoran Bondzio − *Institute of Chemistry and Biochemistry, Freie Universität Berlin, Berlin 14195, Germany*

Oliver Korup − *Department of Chemical Reaction Engineering, Hamburg University of Technology, Hamburg 21073, Germany; Reacnostics GmbH, Hamburg 20457, Germany*

Complete contact information is available at: https://pubs.acs.org/10.1021/acs.iecr.6c01137

Funding

This work was funded by the Hamburgische Investitions- and Förderbank (IFB Hamburg) within the funding scheme "Programm für Innovation (PROFI)—Modul PROFI Transfer Plus" as part of the research project KlAutoMech—Erforschung Kl-basierter Berechnung kinetischer Modelle aus Profil und DRIFTS-Messungen am Use-Case Methanolsynthese. The authors acknowledge additional funding by the Deutsche Forschungsgemeinschaft (DFG, German Research Foundation) − SFB 1615 SMART Reactors− 503850735. Funding by the Einstein Foundation Berlin is also gratefully acknowledged.

Notes

The authors declare no competing financial interest.

■ ACKNOWLEDGMENTS

The authors thank Dr. Wiebke Riedel for the support during IPO-MCP measurements. We thank the TUHH central laboratory for the ICP-OES catalyst characterization. The authors also thank Dr. Patrick Kißling for the assistance with BET catalyst characterization. We acknowledge DESY (Hamburg, Germany), a member of the Helmholtz Association HGF, for providing the experimental facilities for powder XRD measurements. We thank Dr. Gökhan Gizer and Dr. Fernando Igoa for their support with XRD catalyst characterization measurements at P21.1 (Petra III).

■ ABBREVIATIONS

CCU	carbon capture utilization
r-WGS	reverse water−gas shift reaction
CZA	$Cu-ZnO-Al_2O_3$ catalyst
XRD	X-ray diffraction
XAS	X-ray absorption spectroscopy
IR	infrared spectroscopy
DRIFTS	diffuse reflectance infrared Fourier-transform spectroscopy
IPOS	iso-potential operando spectroscopy
MCP	microwave cavity perturbation
FBR	fixed-bed reactor
Q-factor	quality factor
CPR	compact profile reactor
GHSV	gas hourly space velocity
ICP-OES	inductively coupled plasma-optical emission spectroscopy
FID	flame ionization detector.

■ REFERENCES

(1) Genders, S. Sustainable Development Goals UN Global Goals. In *Encyclopedia of Sustainable Management*; Idowu, S. O., Schmidpeter, R., Capaldi, N., Zu, L., Del Baldo, M., Abreu, R., Eds.; Springer International Publishing: Cham, 2023.

(2) Zybert, M. Applied Catalysis in Chemical Industry: Synthesis, Catalyst Design, and Evaluation. *Catalysts* **2023**, *13* (3), 607.

(3) Becka, R.; Bajohr, S.; Kolb, T. Review on CO2 Activation via Catalytic Reverse Water-Gas Shift Reaction. *Chem. Ing. Tech.* **2025**, *97* (8−9), 860−881.

(4) Yamaoka, M.; Tomozawa, K.; Sumiyoshi, K.; Ueda, T.; Ogo, S. Efficient reverse water gas shift reaction at low temperatures over an iron supported catalyst under an electric field. *Sci. Rep.* **2024**, *14* (1), 10216.

(5) Choi, Y.; Sim, G. D.; Jung, U.; Park, Y.; Youn, M. H.; Chun, D. H.; Rhim, G. B.; Kim, K. Y.; Koo, K. Y. Copper catalysts for CO2 hydrogenation to CO through reverse water−gas shift reaction for e-fuel production: Fundamentals, recent advances, and prospects. *Chem. Eng. J.* **2024**, *492*, 152283.

(6) Cui, X.; Kær, S. K. Thermodynamic Analyses of a Moderate-Temperature Process of Carbon Dioxide Hydrogenation to Methanol via Reverse Water−Gas Shift with In Situ Water Removal. *Ind. Eng. Chem. Res.* **2019**, *58* (24), 10559−10569.

(7) Asadi, Z.; Marshall, C. P.; Trunschke, A.; Risse, T. Revealing the Active State of a Cu/ZnO:Al Catalyst During Reverse Water−Gas Shift Reaction in an Operando Microwave Absorption Study. *Angew. Chem., Int. Ed.* **2025**, *64* (46), No. e202504280.

(8) Taniya, K.; Horie, Y.; Fujita, R.; Ichihashi, Y.; Nishiyama, S. Mechanistic study of water−gas shift reaction over copper/zinc-oxide/alumina catalyst in a reformed gas atmosphere: Influence of hydrogen on reaction rate. *Appl. Catal., B* **2023**, *330*, 122568.

(9) Metcalfe, I. S.; Ray, B.; Dejoie, C.; Hu, W.; de Leeuwe, C.; Dueso, C.; García-García, F. R.; Mak, C.-M.; Papaioannou, E. I.; Thompson, C. R.; et al. Overcoming chemical equilibrium limitations

using a thermodynamically reversible chemical reactor. *Nat. Chem.* **2019**, *11* (7), 638−643.
(10) Lohr, T. L.; Lockemeyer, J. R.; Bishopp, S. D.; Motagamwala, A. H.; Wells, G. J.; Wermink, T. Ethylene Oxide: A Catalyst and Process Development Success Story. *Ind. Eng. Chem. Res.* **2024**, *63* (43), 18221−18240.
(11) Schlögl, R. Catalysis 4.0. *ChemCatChem* **2017**, *9* (4), 533−541.
(12) Dave, A. J.; Lee, T.; Ponciroli, R.; Vilim, R. B. Design of a supervisory control system for autonomous operation of advanced reactors. *Ann. Nucl. Energy* **2023**, *182*, 109593.
(13) Becker, T.; Bruns, B.; Lier, S.; Werners, B. Decentralized modular production to increase supply chain efficiency in chemical markets. *J. Bus. Econ.* **2021**, *91* (6), 867−895.
(14) Zhang, L.; Mao, H.; Liu, Q.; Gani, R. Chemical product design − recent advances and perspectives. *Curr. Opin. Chem. Eng.* **2020**, *27*, 22−34.
(15) Bañares, M. A. Operando methodology: combination of in situ spectroscopy and simultaneous activity measurements under catalytic reaction conditions. *Catal. Today* **2005**, *100* (1), 71−77.
(16) Meirer, F.; Weckhuysen, B. M. Spatial and temporal exploration of heterogeneous catalysts with synchrotron radiation. *Nat. Rev. Mater.* **2018**, *3* (9), 324−340.
(17) Wollak, B.; Doronkin, D. E.; Espinoza, D.; Sheppard, T.; Korup, O.; Schmidt, M.; Alizadehfanaloo, S.; Rosowski, F.; Schroer, C.; Grunwaldt, J.-D.; et al. Exploring catalyst dynamics in a fixed bed reactor by correlative operando spatially-resolved structure-activity profiling. *J. Catal.* **2022**, *408*, 372−387.
(18) Kouyate, M.; Ducci, G.; Felsen, F.; Kunkel, C.; Reuter, K.; Scheurer, C. Model driven adaptive design with concentration profiles. *J. Chem. Phys.* **2025**, *163* (22), 224113.
(19) Roldán Cuenya, B.; Bañares, M. A. Introduction: Operando and In Situ Studies in Catalysis and Electrocatalysis. *Chem. Rev.* **2024**, *124* (13), 8011−8013.
(20) Sichert, S.; Stahl, S.-F.; Korup, O.; Horn, R. Measuring Adsorbate Profiles in Heterogeneous Catalytic Reactors by Iso-Potential Operando DRIFTS Applied to CO2Methanation on Ni. *ACS Catal.* **2024**, *14* (11), 8676−8693.
(21) Horn, R. Device and Method for Determination of a Catalyst State in a Chemical Reactor. WO 2021/078817, 2021.
(22) Ovenston, A.; Walls, J. R. AC Electrical Characterization of Heterogeneous Catalysts. *J. Catal.* **1993**, *140* (2), 464−480.
(23) Slater, J. C. Microwave Electronics. *Rev. Mod. Phys.* **1946**, *18* (4), 441−512.
(24) Eichelbaum, M.; Hävecker, M.; Heine, C.; Karpov, A.; Dobner, C.-K.; Rosowski, F.; Trunschke, A.; Schlögl, R. The Intimate Relationship between Bulk Electronic Conductivity and Selectivity in the Catalytic Oxidation of n-Butane. *Angew. Chem., Int. Ed.* **2012**, *51* (25), 6246−6250.
(25) Eichelbaum, M.; Stößer, R.; Karpov, A.; Dobner, C.-K.; Rosowski, F.; Trunschke, A.; Schlögl, R. The microwave cavity perturbation technique for contact-free and in situ electrical conductivity measurements in catalysis and materials science. *Phys. Chem. Chem. Phys.* **2012**, *14* (3), 1302−1312.
(26) Horn, R.; Williams, K. A.; Degenstein, N. J.; Bitsch-Larsen, A.; Dalle Nogare, D.; Tupy, S. A.; Schmidt, L. D. Methane catalytic partial oxidation on autothermal Rh and Pt foam catalysts: Oxidation and reforming zones, transport effects, and approach to thermodynamic equilibrium. *J. Catal.* **2007**, *249* (2), 380−393.
(27) Lin Htun, S.; Goldfarb, J. L. Novel Reactor for In Situ Dielectric Constant Measurements of Fluids at High Temperature and Pressure. *J. Chem. Eng. Data* **2025**, *70* (11), 4471−4482.

https://doi.org/10.1021/acs.iecr.6c01137
Ind. Eng. Chem. Res. XXXX, XXX, XXX−XXX